Synergistic Stabilization of Nucleic Acid Assembly by 2′-*O*,4′-*C*-Methylene-Bridged Nucleic Acid Modification and Additions of Comb-Type Cationic Copolymers[†]

Hidetaka Torigoe,*[,‡] Atushi Maruyama,[§,||] Satoshi Obika,[⊥] Takeshi Imanishi,[⊥] and Takuma Katayama[‡]

Department of Applied Chemistry, Faculty of Science, Tokyo University of Science, 1-3 Kagurazaka, Shinjuku-ku, Tokyo 162-8601, Japan, Division of Integrated Materials, Institute for Materials Chemistry and Engineering, Kyushu University, 744-CE11 Motooka, Nishi-ku, Fukuoka 819-0395, Japan, CREST, Japan Science and Technology Agency, 4-1-8 Honcho, Kawaguchi 332-0012, Japan, and Graduate School of Pharmaceutical Sciences, Osaka University, 1-6 Yamadaoka, Suita, Osaka 565-0871, Japan

Received September 20, 2008; Revised Manuscript Received January 25, 2009

ABSTRACT: Stabilization of nucleic acid assemblies, such as duplex and triplex, is quite important for their wide variety of potential applications. Various stabilization methods, including molecular designs of chemically modified nucleotides and hybrid stabilizers, and combinations of different stabilization methods have been developed to increase stability of nucleic acid assemblies. However, combinations of two stabilizing methods have not always yielded desired synergistic effects. In the present study, to propose a strategy for selection of a rational combination of stabilizing methods, we demonstrate synergistic stabilization of triplex by 2′-*O*,4′-*C*-methylene-bridged nucleic acid (2′,4′-BNA) modification of triplex-forming oligonucleotide and addition of poly(L-lysine)-*graft*-dextran copolymer [poly(L-lysine) grafted with hydrophilic dextran side chains]. Each of these methods increased the binding constant for triplex formation by nearly 2 orders of magnitude. However, their kinetic contributions were quite distinct. The copolymer increased the association rate constant, whereas the 2′,4′-BNA modification decreased the dissociation rate constant for triplex stabilization. The combination of both stabilizing methods increased the binding constant by nearly 4 orders of magnitude. Kinetic analyses revealed that the successful synergistic stabilization resulted from kinetic complementarity between increased association rate constants by the copolymer and decreased dissociation rate constants by the 2′,4′-BNA modification. The stabilizing effect of one stabilization method did not alter that of the other stabilization method. We propose that kinetic analyses of each stabilizing effect permit selection of a rational combination of stabilizing methods for successful synergy in stabilizing nucleic acid assemblies.

Molecular interactions with high specificity are pivotal for chemical and biochemical processes. Base pairing in nucleic acid strands is an outstanding example of such interactions. Watson−Crick base pairing in duplexes and Hoogsteen base pairing in triplexes formed between a single-stranded homopurine or homopyrimidine triplex-forming oligonucleotides (TFO)[1] and homopurine−homopyrimidine stretches in duplexes (*1*−*3*) are involved in sequence-specific nucleic acid interactions. Recently, such assemblies of nucleic acid strands have attracted considerable interest for their wide variety of potential applications in not only life sciences (*4*−*7*) but also nanotechnology including nanomachines and nanodevices (*8*−*10*). In addition to specificity, stability of nucleic acid assemblies is a key factor for their practical utility. Various stabilization methods, including molecular designs of chemically modified nucleotides and hybrid stabilizers for nucleic acid assemblies, have been developed (*11*−*14*). Further stabilization of nucleic acid assemblies has involved combinations of different stabilization methods. However, combinations of two stabilization methods have occasionally resulted in unexpectedly small effects. For example, while each of 2′-*O*,4′-*C*-methylene-bridged nucleic acid (2′,4′-BNA/LNA) modification (*15*−*26*) and N3′→P5′ phosphoramidate modification (*27*−*33*) of nucleic acid strands increases the thermal dissociation temperatures of duplex and triplex significantly, the combination of these two modifications results in less stabilizing activity than the 2′,4′-BNA modification alone (*34, 35*). In another example, while

[†] This research was supported in part by the Grant-in-Aid from the Ministry of Education, Science, Sports, and Culture of Japan (17012022 and 17053027 to H.T., 20240049 to A.M., 18550151 and 20655038 to S.O., and 190390030 to T.I.). H.T. sincerely thanks the Casio Science Promotion Foundation, Nakatani Foundation of Electronic Measuring Technology Advancement, Iketani Science and Technology Foundation, and Kumagai Foundation for Science and Technology. A.M. gratefully acknowledges A3 Foresight Program from JSPS from the Japan Society for the Promotion of Science (JSPS), the Joint Project for Materials Chemistry, and the Global COE Program "Science for Future Molecular Systems" from the Ministry of Education, Culture, Science, Sports, and Technology of Japan.

* To whom correspondence should be addressed. Phone: 81-3-5228-8259. Fax: 81-3-5261-4631. E-mail: htorigoe@rs.kagu.tus.ac.jp.

[‡] Tokyo University of Science.

[§] Kyushu University.

[||] CREST, Japan Science and Technology Agency.

[⊥] Osaka University.

[1] Abbreviations: TFO, triplex-forming oligonucleotide; PLL-*g*-Dex, poly(L-lysine)-*graft*-dextran; 2′,4′-BNA, 2′-*O*,4′-*C*-methylene-bridged nucleic acid; Bt, biotinylated; EMSA, electrophoretic mobility shift assay; T_m, melting temperature; CD, circular dichroism; IAsys, interaction analysis system; k_{on}, on-rate constant; k_{assoc}, association rate constant; k_{off}, off-rate constant; k_{dissoc}, dissociation rate constant.

10.1021/bi801795z CCC: $40.75
Published on Web 01/26/2009

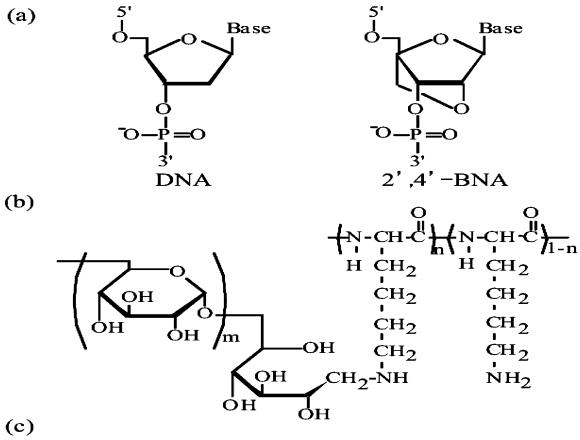


```
Pyr15T              5′-CTCTTCTTTTCTTTC-3′
Pyr15BNA7-1         5′-CTCTTCTTTTCTTTC-3′
Pyr15BNA7-2         5′-CTCTTCTTTTCTTTC-3′
Pyr15BNA5-1         5′-CTCTTCTTTTCTTTC-3′
Pyr15BNA5-2         5′-CTCTTCTTTTCTTTC-3′
Pur23A        5′-GCGCGAGAAGAAAAGAAAGCCGG-3′
Pyr23T        3′-CGCGCTCTTCTTTTCTTTCGGCC-5′
Pyr15NS             5′-TCTCCTCCCCTCCCT-3′
C: C with 2′-O,4′-C-methylene bridge
T: T with 2′-O,4′-C-methylene bridge
```

FIGURE 1: (a) Structural formulas for DNA and 2′,4′-BNA. (b) Structural formula for PLL-*g*-Dex copolymer. The subscript "n" represents the ratio of the number of lysine residues modified by dextran chains to the total number of lysine residues in the copolymer. The subscript "m" represents the number of polymerization degree of dextran. (c) Oligonucleotide sequences for the target duplex (Pur23A·Pyr23T), the specific TFOs (Pyr15T, Pyr15BNA7-1, Pyr15BNA7-2, Pyr15BNA5-1, and Pyr15BNA5-2), and the nonspecific TFO (Pyr15NS).

acridine modification of TFO and addition of a triplex-binding ligand increase the binding constant of triplex formation by 10-fold and 100-fold, respectively, the combination of these two methods results in only a 50-fold increase in triplex stability (*36*). Hence, strategies to select a rational combination of stabilizing methods for successful synergy in stabilizing nucleic acid assemblies are lacking and should be established.

We have previously reported that 2′,4′-BNA modification of TFO (see Figure 1a) increases the binding constant for triplex formation at neutral pH by at least 20-fold (*19, 21*). Kinetic studies have revealed that the increase in binding constant by the 2′,4′-BNA modification results mainly from a considerable decrease in the dissociation rate constant (*19, 21*). In contrast, we have also reported that poly(L-lysine)-*graft*-dextran (PLL-*g*-Dex) copolymer [poly(L-lysine) grafted with hydrophilic dextran side chains; see Figure 1b] significantly increases the stability of duplex (*37*) and triplex (*38*−*45*) by reducing counterion condensation effects. This copolymer increases the binding constant for triplex formation at neutral pH by nearly 2 orders of magnitude (*41, 42*). Kinetic studies have demonstrated that the increase in binding constant by the copolymer results from a considerable increase in the association rate constant rather than a decrease in the dissociation rate constant (*41, 42*). The kinetic effect of addition of the copolymer is in sharp contrast with that of the 2′,4′-BNA modification of TFO. The difference in the kinetic effects between addition of the copolymer and the 2′,4′-BNA modification of TFO produced our hypothesis that the copolymer should further increase stability of triplexes involving the 2′,4′-BNA-modified TFO.

In the present study, we demonstrate that the combinations of these two stabilizing methods synergistically increase the binding constant for triplex formation at neutral pH. Kinetic analyses reveal that observed stabilization results from kinetic complementarity between increased association rate constants by the copolymer and decreased dissociation rate constants by the 2′,4′-BNA modification of TFO. No countering interference between these stabilizing effects was observed. We propose that kinetic analyses of each stabilizing effect permit selection of a rational combination of stabilizing methods for successful synergy in stabilizing nucleic acid assemblies.

MATERIALS AND METHODS

Preparation of Oligonucleotides. We synthesized 23-mer complementary oligonucleotides for a target duplex, Pur23A and Pyr23T (Figure 1c), a 15-mer unmodified homopyrimidine TFO specific for the target duplex, Pyr15T (Figure 1c), and a nonspecific homopyrimidine oligonucleotide, Pyr15NS (Figure 1c), on an ABI DNA synthesizer using the solid-phase cyanoethyl phosphoramidite method and purified them with a reverse-phase high-performance liquid chromatography (HPLC) on a Wakosil DNA column. The 15-mer 2′,4′-BNA-modified homopyrimidine TFOs, Pyr15BNA7-1, Pyr15BNA7-2, Pyr15BNA5-1, and Pyr15BNA5-2 (Figure 1c), were synthesized and purified as described previously (*16, 17, 20*). 5′-Biotinylated Pyr23T (denoted as Bt-Pyr23T) was prepared using biotin phosphoramidite. The concentration of all oligonucleotides was determined by UV absorbance. Complementary strands, Pur23A and Pyr23T, were annealed by heating at up to 90 °C, followed by a gradual cooling to room temperature. The annealed sample was applied on a hydroxyapatite column (Bio-Rad Inc.) to remove unpaired single strands. The concentration of the duplex DNA (Pur23A·Pyr23T) was determined by UV absorption considering the DNA concentration ratio of 1 OD = 50 μg/ml, with a M_r of 15180.

Preparation of the PLL-g-Dex Copolymer. The PLL-*g*-Dex copolymer (number average molecular weight = 1.68 × 10^4, dextran content = 81.8 wt %, Figure 1b) was prepared by a reductive amination reaction between poly (L-lysine) and dextran T-10, as described in detail previously (*37, 38*). Dextran content >80 wt % is required to obtain totally soluble complex with DNA. These copolymers do not trigger DNA condensation, which likely interferes with DNA/DNA interaction (*37, 46*). Further increase in dextran content >95 wt % may result in reduced interaction between DNA and the polycationic backbone, leading to loss in copolymer's efficacy for triplex stabilization. The copolymer structure in the present study is not optimized for triplex stabilization purpose but roughly optimized to obtain the complex with suitable properties.

Electrophoretic Mobility Shift Assay (EMSA). EMSA experiments were performed as described in detail previously by a 15% native polyacrylamide gel electrophoresis (*19, 33, 39*−*41, 47*).

UV Melting. UV melting experiments were carried out on a DU-640 spectrophotometer (Beckman Inc.) equipped with a Peltier-type cell holder. Cell path length was 1 cm. UV melting profiles were measured in buffer A (10 mM sodium cacodylate−cacodylic acid at pH 6.8 containing 200 mM

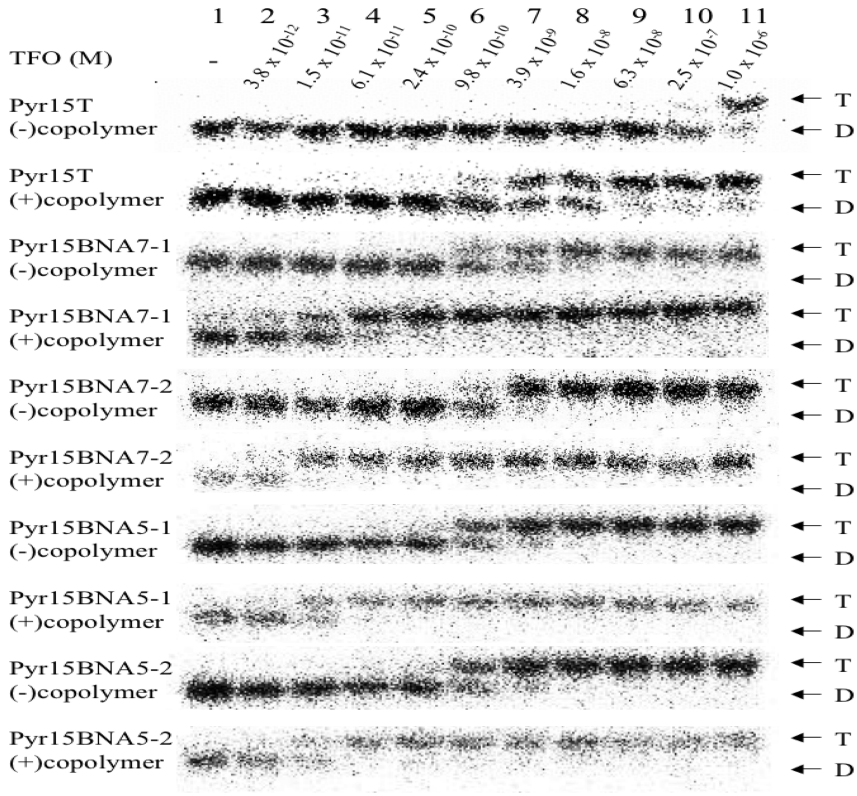

FIGURE 2: EMSA results for triplex formation involving Pyr15T, Pyr15BNA7-1, Pyr15BNA7-2, Pyr15BNA5-1, or Pyr15BNA5-2 at neutral pH with or without addition of PLL-*g*-Dex copolymer. Triplex formation was initiated by adding ^{32}P-labeled Pur23A·Pyr23T duplex (1 fmol) with the indicated final concentrations of Pyr15T, Pyr15BNA7-1, Pyr15BNA7-2, Pyr15BNA5-1, or Pyr15BNA5-2. Pyr15NS was added to adjust the equimolar concentrations (10 μM) of TFO (Pyr15T + Pyr15NS, Pyr15BNA7-1 + Pyr15NS, Pyr15BNA7-2 + Pyr15NS, Pyr15BNA5-1 + Pyr15NS, or Pyr15BNA5-2 + Pyr15NS) in each lane. Reaction mixtures involving Pyr15T, Pyr15BNA7-1, Pyr15BNA7-2, Pyr15BNA5-1, or Pyr15BNA5-2 in buffer [50 mM Tris−acetate (pH 7.0), 100 mM sodium chloride, and 10 mM magnesium chloride] with or without 11.7 μM PLL-*g*-Dex copolymer (charge ratio of $[\text{amino groups}]_{\text{copolymer}}/[\text{phosphate groups}]_{\text{DNA}} = 2$) were incubated for 6 h at 37 °C to ensure the equilibrium of the triplex formation and then electrophoretically separated on a 15% native polyacrylamide gel at 4 °C. Positions of the duplex (D) and triplex (T) are indicated.

NaCl and 20 mM $MgCl_2$) with or without 4.85 μM PLL-*g*-Dex copolymer at a scan rate of 0.5 °C/min at 260 nm. The first derivative was calculated from the UV melting profile. The peak temperatures in the derivative curve were designated as the melting temperature, T_m. The triplex nucleic acid concentration used was 1 μM.

CD Spectroscopy. CD spectra at 25 °C were recorded in buffer A (see UV melting) with or without 4.85 μM PLL-*g*-Dex copolymer on a JASCO J-720 spectropolarimeter interfaced with a microcomputer. Cell path length was 1 cm. The triplex nucleic acid concentration used was 1 μM.

Kinetic Analyses by Resonant Mirror Method. Kinetic experiments by resonant mirror method on an IAsys plus instrument (Affinity Sensors Cambridge Inc.) were performed as described in detail previously, where a real-time biomolecular interaction was measured with a laser biosensor (*19, 33, 41, 47*−*49*).

RESULTS

Electrophoretic Mobility Shift Assay (EMSA) of Triplex Formation at Neutral pH. Triplex formation of the target duplex, Pur23A·Pyr23T (Figure 1c), with TFO, Pyr15T (Figure 1c) or each of the 2′,4′-BNA-modified TFO (Pyr15BNA7-1, Pyr15BNA7-2, Pyr15BNA5-1, or Pyr15BNA5-2) (Figure 1c), was examined either with or without added PLL-*g*-Dex copolymer (Figure 1b) at pH 7.0 by EMSA (Figure 2). Total oligonucleotide concentration ([specific TFO (Pyr15T, Pyr15BNA7-1, Pyr15BNA7-2, Pyr15BNA5-1, or Pyr15BNA5-2; Figure 1c)] + [nonspecific oligonucleotide (Pyr15NS; Figure 1c)]) was kept constant at 10 μM to achieve equal charge ratios of $[\text{amino groups}]_{\text{copolymer}}/[\text{phosphate groups}]_{\text{DNA}}$ and to assess sequence specificity. Incubation with Pyr15T, Pyr15BNA7-1, Pyr15BNA7-2, Pyr15BNA5-1, or Pyr15BNA5-2 at specific concentrations caused retardation of duplex migration due to triplex formation (*19, 33, 39*−*41, 47*). The percentage of the formed triplex was calculated using the equation:

$$\%\ \text{triplex} = [S_{\text{triplex}}/(S_{\text{triplex}} + S_{\text{duplex}})] \times 100$$

where S_{triplex} and S_{duplex} represent the radioactive signal for triplex and duplex bands, respectively. The dissociation constant, K_d, for triplex formation was determined from the concentration of the TFO, producing 50% conversion of duplex to triplex (*19, 33, 39*−*41, 47*). The K_d for the triplex involving Pyr15T without the copolymer [Pyr15T, (−) copolymer] was estimated to be $\sim 10^{-7}$ M. In contrast, the K_d for the triplex involving Pyr15T with the copolymer [Pyr15T, (+) copolymer] was $\sim 10^{-9}$ M, indicating that the copolymer increases triplex stability by nearly 2 orders of magnitude. Incubation with 10 μM Pyr15NS (nonspecific oligonucleotide) alone in the presence of the copolymer did not shift electrophoretic migration of the target duplex [see lane 1, (+) copolymer], indicating that the copolymer preserved sequence specificity of triplex formation. On the

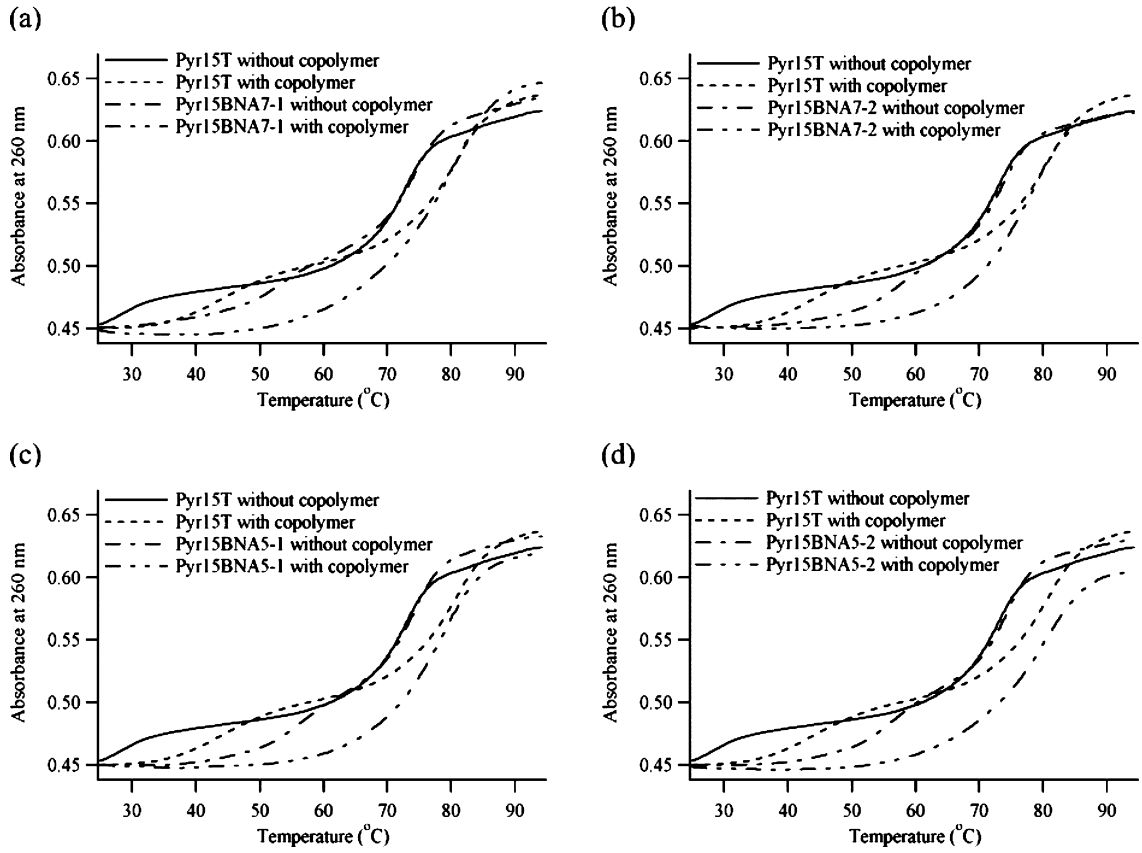

FIGURE 3: UV melting profiles for the triplex involving Pyr15T (a−d), Pyr15BNA7-1 (a), Pyr15BNA7-2 (b), Pyr15BNA5-1 (c), or Pyr15BNA5-2 (d) at neutral pH with or without the PLL-*g*-Dex copolymer. Triplexes involving Pyr15T, Pyr15BNA7-1, Pyr15BNA7-2, Pyr15BNA5-1, or Pyr15BNA5-2 in buffer A (see Materials and Methods) with or without 4.85 μM PLL-*g*-Dex copolymer (the charge ratio of $[\text{amino groups}]_{\text{copolymer}}/[\text{phosphate groups}]_{\text{DNA}} = 2$) were melted at a scan rate of 0.5 °C/min with detection at 260 nm.

other hand, the K_d for the triplex involving each of the 2′,4′-BNA-modified TFO without the copolymer [Pyr15BNA7-1, (−) copolymer; Pyr15BNA7-2, (−) copolymer; Pyr15BNA5-1, (−) copolymer; Pyr15BNA5-2, (−) copolymer] was $\sim 10^{-9}$ M, indicating that the 2′,4′-BNA modification increases triplex stability by nearly 2 orders of magnitude. The increase in the triplex stability by the 2′,4′-BNA modification was similar in magnitude among the four modified TFOs. We then assessed cooperativity between the copolymer and the 2′,4′-BNA modification [Pyr15BNA7-1, (+) copolymer; Pyr15BNA7-2, (+) copolymer; Pyr15BNA5-1, (+) copolymer; Pyr15BNA5-2, (+) copolymer]. Note that triplex formation, even at TFO concentration of 10^{-11} M, was observed for each of the 2′,4′-BNA-modified TFO with the copolymer, demonstrating nearly a 10^4-fold increase in the triplex stability by combining these stabilizing strategies.

Spectroscopic Characterization of Triplex Formation at Neutral pH. Thermal stability of the triplex involving TFO, Pyr15T or each of the 2′,4′-BNA-modified TFO (Pyr15BNA7-1, Pyr15BNA7-2, Pyr15BNA5-1, or Pyr15BNA5-2), was investigated either with or without the PLL-*g*-Dex copolymer at pH 6.8 by UV melting measurements (Figure 3 and Table 1). The triplex involving Pyr15T without the copolymer exhibited a biphasic thermal dissociation profile. The first transition at lower temperature, T_{m1}, was attributed to the thermal dissociation of triplex to duplex and a TFO. The second transition at higher temperature, T_{m2}, was the melting of the duplex. Addition of the copolymer to the triplex involving Pyr15T increased both T_{m1} and T_{m2}, respectively, indicating that the copolymer increased the thermal stability

Table 1: Melting Temperatures of 1 μM Triplexes Involving Pyr15T, Pyr15BNA7-1, Pyr15BNA7-2, Pyr15BNA5-1, or Pyr15BNA5-2 with or without 4.85 μM PLL-*g*-Dex Copolymer at pH 6.8 in Buffer A (See Materials and Methods), Obtained from UV Melting

TFO	PLL-*g*-Dex copolymer	T_{m1} (°C)	T_m (°C)	T_{m2} (°C)
Pyr15T	−	28.4 ± 0.7		72.3 ± 0.6
Pyr15T	+	44.3 ± 1.2		80.4 ± 0.5
Pyr15BNA7-1	−	53.5 ± 0.3		73.9 ± 0.5
Pyr15BNA7-1	+		80.4 ± 0.3[a]	
Pyr15BNA7-2	−	57.8 ± 0.9		74.1 ± 1.4
Pyr15BNA7-2	+		79.1 ± 2.8[a]	
Pyr15BNA5-1	−	56.7 ± 1.1		74.1 ± 1.7
Pyr15BNA5-1	+		79.5 ± 2.6[a]	
Pyr15BNA5-2	−	57.1 ± 0.9		74.2 ± 0.6
Pyr15BNA5-2	+		79.7 ± 2.5[a]	

[a] One-step transition corresponds to a direct thermal dissociation of the triplex to its constituent single strands.

of both the triplex and duplex. On the other hand, T_{m1} without the copolymer for each of the 2′,4′-BNA-modified TFO (Pyr15BNA7-1, Pyr15BNA7-2, Pyr15BNA5-1, or Pyr15BNA5-2) was significantly higher than that for Pyr15T, although T_{m2} without the copolymer was almost identical among all the triplexes. Thus, the 2′,4′-BNA modification increased the thermal stability of only the triplex. Next, we evaluated the effect of the copolymer on the thermal stability of the triplex involving each of the 2′,4′-BNA-modified TFO. The triplex involving each of Pyr15BNA7-1, Pyr15BNA7-2, Pyr15BNA5-1, or Pyr15BNA5-2 with the copolymer exhibited only one transition at higher temperature, T_m. As the UV absorbance change at T_m under this condition was nearly equal to the sum of those at T_{m1} and T_{m2}, the transition was identified as

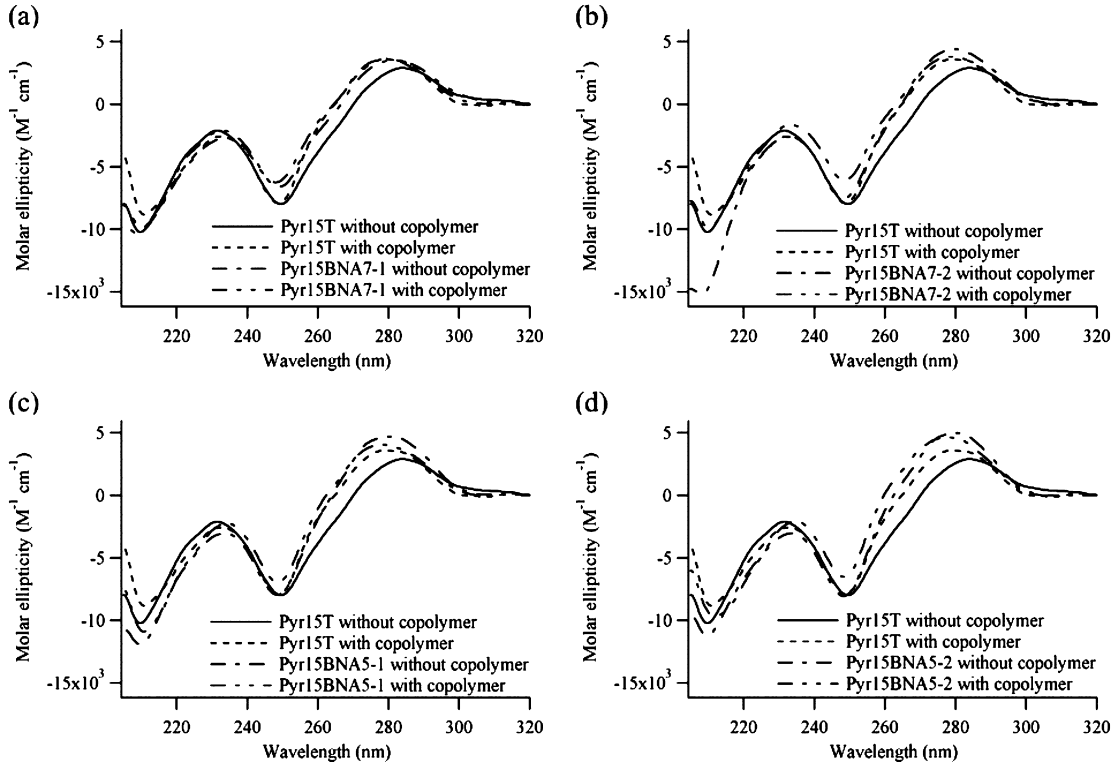

FIGURE 4: CD spectra for the triplex involving Pyr15T (a−d), Pyr15BNA7-1 (a), Pyr15BNA7-2 (b), Pyr15BNA5-1 (c), or Pyr15BNA5-2 (d) at neutral pH with or without the PLL-*g*-Dex copolymer. The triplexes involving Pyr15T, Pyr15BNA7-1, Pyr15BNA7-2, Pyr15BNA5-1, or Pyr15BNA5-2 at 25 °C and pH 6.8 in buffer A (see Materials and Methods) with or without 4.85 μM PLL-*g*-Dex copolymer (the charge ratio of $[\text{amino groups}]_{\text{copolymer}}/[\text{phosphate groups}]_{\text{DNA}} = 2$) were measured in the wavelength range of 205−320 nm.

a direct thermal dissociation of the triplex to its constituent single strands. Therefore, the copolymer further increased the thermal stability of the triplex involving Pyr15BNA7-1, Pyr15BNA7-2, Pyr15BNA5-1, or Pyr15BNA5-2 by more than 20 °C without affecting the hyperchromicity, indicating that the copolymer and the 2′,4′-BNA modification cooperatively increased the thermal stability of the triplex.

Triplexes involving Pyr15T or each of the 2′,4′-BNA-modified TFO (Pyr15BNA7-1, Pyr15BNA7-2, Pyr15BNA5-1, or Pyr15BNA5-2) either with or without the PLL-*g*-Dex copolymer were further characterized by CD spectra measurements (Figure 4). The CD profiles at 25 °C and pH 6.8 were similar for all the different conditions, confirming triplex formation involving Pyr15T or each of the 2′,4′-BNA-modified TFO either with or without the copolymer (*50*). No significant change in highly ordered triplex structure by either the copolymer or the 2′,4′-BNA modification was observed.

Kinetic Analyses of Triplex Formation at Neutral pH. To understand the stabilization cooperativity observed between PLL-*g*-Dex copolymer and 2′,4′-BNA modification (Figures 2 and 3), the kinetic parameters for the association and dissociation of TFO (Pyr15T, Pyr15BNA7-1, Pyr15BNA7-2, Pyr15BNA5-1, or Pyr15BNA5-2) with Pur23A•Pyr23T were assessed either with or without the PLL-*g*-Dex copolymer at 25 °C and pH 6.8 by IAsys surface affinity measurements (Figure 5). Figure 5a compares the sensorgrams representing triplex formation and dissociation involving 2 μM specific TFO with or without the copolymer. Pyr15T over the immobilized Bt-Pyr23T•Pur23A caused an increase in sensor response. The response was more substantially increased when the same measurement was performed in the presence of the copolymer, indicating that the copolymer significantly increased the association rate constant for the triplex. In contrast, although the change in the association curve was moderately enhanced by Pyr15BNA7-2 in the absence of the copolymer, the change in the dissociation curve over time for Pyr15BNA7-2 was much smaller than that for Pyr15T. These results indicate that the 2′,4′-BNA modification remarkably decreased the dissociation rate constant for the triplex. Note that both intrinsic effects from the copolymer and the 2′,4′-BNA modification were apparent in both association and dissociation curves for Pyr15BNA7-2 in the presence of the copolymer. The similar profiles were obtained for Pyr15BNA7-1, Pyr15BNA5-1, and Pyr15BNA5-2. Combination of the copolymer and the 2′,4′-BNA modification thus permitted rapid formation of a durable triplex.

To explore these kinetic effects more quantitatively, we analyzed a series of association and dissociation curves as a function of TFO concentration. As shown in Figure 5b, increasing concentrations of Pyr15BNA7-2 produces a gradual change in the association curves. On-rate constants (k_{on}) obtained from the analysis of each association curve are shown in Figure 5c plotted against Pyr15BNA7-2 concentrations. The association rate constant (k_{assoc}) was determined from the slope of the fitted line obtained by a linear least-squares method (*19, 33, 41, 47*−*49*). The off-rate constant (k_{off}) was obtained from analysis of each dissociation curve (Figure 5a; data not shown). Because k_{off} is usually independent of the solution concentration, the dissociation rate constant (k_{dissoc}) was determined by averaging k_{off} for several concentrations (*19, 33, 41, 47*−*49*). The binding constant, K_a, was calculated from $K_a = k_{\text{assoc}}/k_{\text{dissoc}}$. All kinetic parameters obtained under various conditions were summarized in Table 2. Magnitudes of K_a determined from the kinetic study (Table 2) were consistent with those

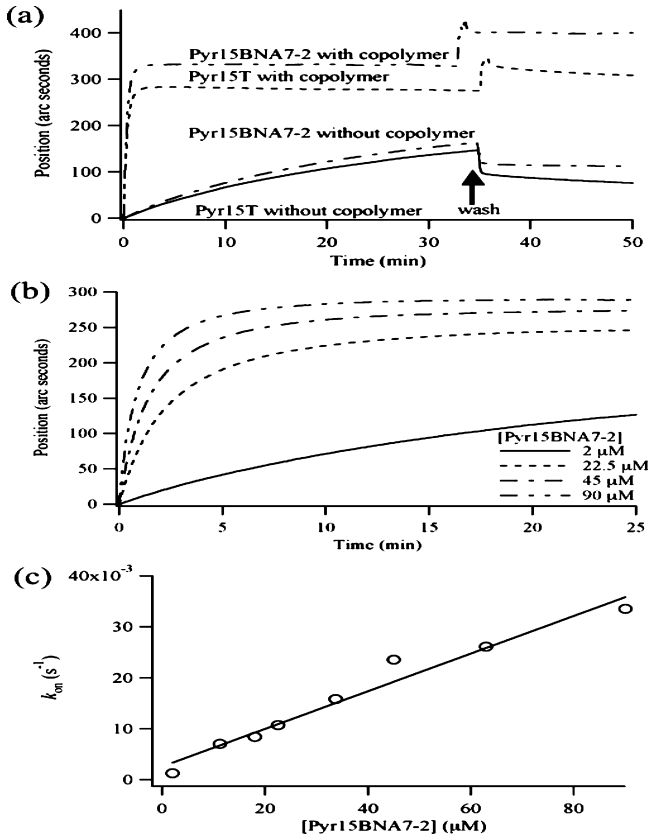

FIGURE 5: Kinetic analyses for triplex formation involving Pyr15T or Pyr15BNA7-2 at pH 6.8 in buffer A (see Materials and Methods) with or without the PLL-*g*-Dex copolymer. (a) Typical sensorgrams for triplex formation at 25 °C and pH 6.8 after injecting 2 μM TFO (Pyr15T or Pyr15BNA7-2) with or without 44.6 μM PLL-*g*-Dex copolymer into the Bt-Pyr23T·Pur23A-immobilized cuvette are shown. (b) A series of sensorgrams for triplex formation between Pyr15BNA7-2 and Pur23A·Pyr23T at 25 °C and pH 6.8 without the copolymer. The Pyr15BNA7-2 solutions, diluted in buffer A to achieve the indicated final concentrations, were injected into the Bt-Pyr23T·Pur23A-immobilized cuvette. Binding of Pyr15BNA7-2 to Bt-Pyr23T·Pur23A was monitored over time. (c) The on-rate constants, k_{on}, obtained from panel b were plotted against the respective concentrations of Pyr15BNA7-2. The plot was fit to a straight line ($r^2 = 0.98$) by linear least-squares method.

obtained from EMSA (Figure 2). Either the copolymer or the 2′,4′-BNA modification increased K_a by nearly 50-fold. However, their kinetic contributions were quite distinct. The copolymer increased k_{assoc} by about 45-fold, while decreasing k_{dissoc} by 1.5-fold. In contrast to the copolymer, the 2′,4′-BNA modification decreased k_{dissoc} by about 50-fold, while it moderately decreased k_{assoc} by 1.2-fold. The combination of the copolymer and the 2′,4′-BNA modification resulted in a more than 2000-fold increase in K_a. By comparing the kinetic parameters, we note that k_{assoc} and k_{dissoc} obtained for Pyr15BNA7-2 with the copolymer closely coincide with the mathematical products of values individually obtained for either Pyr15T with the copolymer or Pyr15BNA7-2 without the copolymer. Consequently, results clearly demonstrate that mutual kinetic influences successfully cooperate to stabilize triplex formation without generating negative interference.

DISCUSSION

The PLL-*g*-Dex copolymer increased K_a for the triplex formation at pH 6.8 and 25 °C by nearly 2 orders of magnitude (Figures 2 and 5 and Table 2). The copolymer also increased T_m for the triplex (Figure 3 and Table 1). These results indicate that the PLL-*g*-Dex copolymer significantly stabilizes the triplex at neutral pH, consistent with our previous results (*39*−*42*). Entropic loss due to counterion condensation and electrostatic repulsion caused by excess accumulation of phosphate negative charges upon triplex formation usually produces the instability of triplex (*51*−*53*). Therefore, cationic substances, such as polyamines, are employed to stabilize triplex (*54, 55*). Spermine, bearing four positive charges, stabilizes triplex under low ionic strength (*54, 55*). However, its stabilizing effect is drastically reduced by increasing ionic strength to physiological levels due to competitive replacement of spermine with coexisting cations (*55*). Our previous study (*39*−*42*) and the present results described above demonstrate that the PLL-*g*-Dex copolymer maintains its stabilizing efficacy even under physiological ionic strength through polyvalent electrostatic interactions. Reduced counterion condensation, causing a net increase in entropy change, may increase K_a (*43, 56, 57*). As shown in the CD spectra (Figure 4), the copolymer did not change highly ordered structure of the triplex in spite of stable association, whereas structural changes have been commonly observed for complexes between DNA and cationic homopolymers, such as poly (L-lysine) (*58*−*60*). Preservation of highly ordered structure of triplex may be important for conserving sequence-specific interactions between TFO and the target duplex. Increased K_a by the copolymer resulted mainly from the increase in k_{assoc} rather than the decrease in k_{dissoc} (Table 2), consistent with our previous study (*41, 42*). The reason why the copolymer increases k_{assoc} rather than decreasing k_{dissoc} is unclear. It may be plausible that the copolymer facilitates nucleation of TFO with the target duplex to accelerate triplex formation. Our observation (*61*−*63*) that the copolymer considerably accelerates strand exchange reactions between duplex DNA and its complementary single-stranded DNA may support this consideration. Nucleation complexes consisting of three strands are likely involved in transition states for both triplex formation and strand exchange reactions. It seems that the copolymer is capable of stabilizing not only matured triplex but also three-stranded nucleation complexes by reducing counterion condensation effects. We have recently evaluated the salt dependence on association rate of duplex formation (*64*). In the absence of the copolymer, the association rate increased linearly with log [NaCl], indicating that the counterion associating process is involved in the rate-determining process, presumably nucleation step, of duplex formation. In the presence of the copolymer the association rate is increased 2−3 orders, but no salt dependence was observed. This strongly indicated that reduction of counterion condensation effect is involved in the acceleration effect of the copolymer. We also speculate that the acceleration of triplex formation observed in this work is explainable by the same mechanism. On the other hand, molecular crowding effect needs usually >20 wt % solution of polymers. The polymer concentration in this study is 0.01−0.1 wt %, which is out of the range where so-called molecular crowding effect takes place. We do not think that the molecular crowding effect is a major mechanism to explain our observation.

To discuss the triplex stabilization by the copolymer, the charge ratio of amino groups of the copolymer [amino groups]$_{copolymer}$ to phosphate groups of DNA [phosphate

Table 2: Kinetic Parameters for Triplex Formation Involving Pyr15T or Pyr15BNA7-2 with or without 44.6 μM PLL-*g*-Dex Copolymer in Buffer A (See Materials and Methods) at 25 °C and pH 6.8, Obtained from IAsys Surface Affinity Assay

TFO	PLL-*g*-Dex copolymer	k_{assoc} (M^{-1} s^{-1})	k_{assoc} (relative)	k_{dissoc} (s^{-1})	k_{dissoc} (relative)	K_a (M^{-1})	K_a (relative)
Pyr15T	−	$(6.31 \pm 0.18) \times 10^2$	1.0	$(1.17 \pm 0.14) \times 10^{-2}$	1.0	$(5.41 \pm 0.91) \times 10^4$	1.0
Pyr15T	+	$(2.88 \pm 0.23) \times 10^4$	45.6	$(7.8 \pm 3.4) \times 10^{-3}$	0.67	$(3.69 \pm 1.32) \times 10^6$	68.2
Pyr15BNA7-2	−	$(5.05 \pm 0.77) \times 10^2$	0.80	$(2.35 \pm 3.07) \times 10^{-4}$	0.020	$(2.15 \pm 1.36) \times 10^6$	39.7
Pyr15BNA7-2	+	$(2.48 \pm 0.55) \times 10^4$	39.3	$(2.24 \pm 3.43) \times 10^{-4}$	0.019	$(1.11 \pm 0.77) \times 10^8$	2050

groups]$_{DNA}$ is more important than the molar concentration ratio of the copolymer to DNA. The concentration of amino groups of 4.85 μM copolymer used for the UV melting is 115.9 μM, based on the following calculation, 4.85 μM × [molecular weight of the copolymer: 1.68×10^4] × [wt % of the poly(L-lysine): (100 − 81.8)/100] ÷ [molecular weight of L-lysine: 128] = 115.9 μM. The concentration of phosphate groups of 1 μM triplex used for the UV melting is 58 μM based on the following calculation, 1 μM × [number of phosphate groups of TFO and the target duplex: (15 − 1) + (23 − 1) × 2] = 58 μM. Thus, the charge ratio of [amino groups]$_{copolymer}$/[phosphate groups]$_{DNA}$ is 2 for the UV melting, as shown in the legend of Figure 3. On the other hand, the concentration of amino groups of 44.6 μM copolymer used for the kinetic analyses is 1066 μM, based on the same calculation described above. Concentration of phosphate groups for the kinetic analyses is mainly determined by the concentration of phosphate groups of TFO, because the molar concentration of the added TFO was significantly larger than that of the immobilized trace amount of the target duplex. Because the molar concentration of the added TFO was 11.25−90 μM, the concentration of phosphate groups of TFO was 158−1260 μM, based on the similar calculation described above. Thus, the charge ratio of [amino groups]$_{copolymer}$/[phosphate groups]$_{DNA}$ is 0.85−6.7 for the kinetic analyses. Based on these considerations, the charge ratio of [amino groups]$_{copolymer}$/[phosphate groups]$_{DNA}$ important for the triplex stabilization by the copolymer was not significantly different between the UV melting (the charge ratio = 2) and the kinetic analyses (the charge ratio = 0.85−6.7). We believe that no significant difference in the charge ratio alters the triplex properties.

The 2′,4′-BNA modification increased K_a for the triplex formation at pH 6.8 and 25 °C by nearly 2 orders of magnitude (Figures 2 and 5 and Table 2). This stabilization effect by the 2′,4′-BNA modification was also demonstrated by T_m measurements (Figure 3 and Table 1). These results indicate that 2′,4′-BNA modification significantly stabilizes the triplex at neutral pH, consistent with our previous results (*18*−*21*). The 2′,4′-BNA modification significantly decreased k_{dissoc} to increase K_a (Table 2). The kinetic effect of the 2′,4′-BNA modification is in sharp contrast with that of the PLL-*g*-Dex copolymer described above. The stabilization mechanism for the 2′,4′-BNA modification should be, therefore, distinct from that for the copolymer. Our previous isothermal titration calorimetry study showed that the magnitude of negative ΔS at 25 °C for triplex formation involving 2′,4′-BNA-modified TFO was significantly smaller than that involving unmodified TFO (*19, 21*). Because the source of the negative ΔS for triplex formation was proposed to be due to conformational restraints of TFO involved in triplex formation (*65*), the smaller magnitude of the negative ΔS for 2′,4′-BNA-modified TFO suggests that 2′,4′-BNA-modified TFO in its free state may be more rigid than the corresponding unmodified TFO. This rigidity of 2′,4′-BNA-modified TFO causes a smaller entropic loss upon triplex formation, providing a favorable component to K_a and ΔG and leading to increased K_a. The increase in K_a (Figure 2) and T_m (Figure 3 and Table 1) by the 2′,4′-BNA modification was similar in magnitude among the four modified TFOs, indicating that the number and position of 2′,4′-BNA modification did not significantly affect the extent of the increased stability. The rigidity itself of 2′,4′-BNA-modified TFO may be more important to achieve the increased stability than the variation of the number and position of 2′,4′-BNA modification. We have previously reported the T_m values of triplexes containing different number of 2′,4′-BNA modifications (*66*). Even a single modification increased the T_m value of the triplex. Increasing the number of the modifications from one to three further increased the T_m value of the triplex. The T_m value of the triplex containing three continuous modifications was found to decrease compared with that containing three interrupted modifications. Continuous 2′,4′-BNA modifications were less favorable for the triplex stabilization than the same number of modifications located apart from each other. The T_m values of the triplex with five or seven modifications were higher than those with three or four modifications. Taken together, even lesser number of 2′,4′-BNA modifications has the ability to stabilize the triplex, but the degree of the triplex stabilization may be decreased. As shown in the CD spectra (Figure 4), the 2′,4′-BNA modification did not alter highly ordered structure of the triplex in spite of stable association. Preservation of highly ordered structure of triplex may be important for conserving sequence-specific interactions between TFO and the target duplex. However, the detailed stabilization mechanism for the 2′,4′-BNA modification remains to be elucidated.

The combination of the copolymer and the 2′,4′-BNA modification increased K_a for the triplex formation at pH 6.8 and 25 °C by about 4 orders of magnitude (Figures 2 and 5 and Table 2). This cooperative effect was also confirmed by T_m measurements (Figure 3 and Table 1). The increase in K_a resulted mainly from increased k_{assoc} by the copolymer and decreased k_{dissoc} by the 2′,4′-BNA modification (Table 2). Note that k_{assoc} and k_{dissoc} observed for synergistic effects of both the copolymer and the 2′,4′-BNA modification closely coincided with the mathematical products of the values obtained individually (Table 2). These results clearly demonstrate that neither interference nor negative cooperation between their mutual kinetic effects complicated the synergism.

Different combinations of various stabilizing methods have attempted to produce cooperative stabilization of nucleic acid assembly. Simple combinations of two stabilizing methods have not always yielded the desired cooperative effects. For example, each of the 2′,4′-BNA modification (*16*−*21*) and

the N3′→P5′ phosphoramidate modification (*27*−*33*) increased T_m for both duplex and triplex significantly. However, thermal stability for both duplex and triplex produced by the combination of these two modifications was lower than that by the 2′,4′-BNA modification alone (*34*). Strand interference and no cooperativity of the two stabilizing methods occurred. Both the 2′,4′-BNA modification and the N3′→P5′ phosphoramidate modification seemingly constrain nucleotide conformation, so that their cooperative effects may be difficult. Our previous kinetic studies revealed that both of these modifications decreased k_{dissoc} to increase K_a (*19, 21, 33*), demonstrating that these modifications contribute similarly to the kinetics of nucleic acid assembly. Negative cooperativity between two triplex-stabilizing methods was also reported for combination of acridine-modified TFO and a triplex-binding ligand (*36*). In contrast, in the present study as well as a previous study (*47*), we report synergistic stabilization effects produced by combination of the copolymer and the 2′,4′-BNA or N3′→P5′ phosphoramidate modification. The N3′→P5′ modification increased k_{assoc} for the increase in K_a, but the 2′,4′-BNA modification decreased k_{assoc} in spite of the increase in K_a. Although the effect on k_{assoc} is quite different between the N3′→P5′ modification and the 2′,4′-BNA modification, the synergic stabilization effects by combination with the copolymer were successfully achieved. Kinetic complementarity between increased k_{assoc} by the copolymer and decreased k_{dissoc} by the 2′,4′-BNA or N3′→P5′ phosphoramidate modification may enable the synergistic stabilization effects. Taken together, we propose that kinetic analyses of each stabilizing effect permit selection of a rational combination of stabilizing methods for successful synergy in stabilizing nucleic acid assemblies.

REFERENCES

1. Soyfer, V. N., and Potaman, V. N. (1996) *Triple-Helical Nuleic Acids*, Springer-Verlag, New York.
2. Ghosh, I., Stains, C. I., Ooi, A. T., and Segal, D. J. (2006) Direct detection of double-stranded DNA: Molecular methods and applications for DNA diagnostics. *Mol. Biosyst. 2*, 551–560.
3. Jain, A., Wang, G., and Vasquez, K. M. (2008) DNA triple helices: Biological consequences and therapeutic potential. *Biochimie 90*, 1117–1130.
4. Zhang, C., Pei, J., Kumar, D., Sakabe, I., Boudreau, H. E., Gokhale, P. C., and Kasid, U. N. (2007) Antisense oligonucleotides: target validation and development of systemically delivered therapeutic nanoparticles. *Methods Mol. Biol. 361*, 163–185.
5. Isaka, Y. (2007) DNAzymes as potential therapeutic molecules. *Curr. Opin. Mol. Ther. 9*, 132–136.
6. Missailidis, S., and Perkins, A. (2007) Update: aptamers as novel radiopharmaceuticals: their applications and future prospects in diagnosis and therapy. *Cancer Biother. Radiopharm. 22*, 453–468.
7. Peek, A. S., and Behlke, M. A. (2007) Design of active small interfering RNAs. *Curr. Opin. Mol. Ther. 9*, 110–118.
8. Fink, H. W., and Schonenberger, C. (1999) Electrical conduction through DNA molecules. *Nature 398*, 407–410.
9. Kelley, S. O., and Barton, J. K. (1999) Electron transfer between bases in double helical DNA. *Science 283*, 375–381.
10. Porath, D., Bezryadin, A., de Vries, S., and Dekker, C. (2000) Direct measurement of electrical transport through DNA molecules. *Nature 403*, 635–638.
11. Sahu, N. K., Shilakari, G., Nayak, A., and Kohli, D. V. (2007) Antisense technology: a selective tool for gene expression regulation and gene targeting. *Curr. Pharm. Biotechnol. 8*, 291–304.
12. Wojciechowski, F., and Hudson, R. H. (2007) Nucleobase modifications in peptide nucleic acids. *Curr. Top. Med. Chem. 7*, 667–679.
13. Corradini, R., Sforza, S., Tedeschi, T., Totsingan, F., and Marchelli, R. (2007) Peptide nucleic acids with a structurally biased backbone: effects of conformational constraints and stereochemistry. *Curr. Top. Med. Chem. 7*, 681–694.
14. Faria, M., and Ulrich, H. (2008) Sugar boost: when ribose modifications improve oligonucleotide performance. *Curr. Opin. Mol. Ther. 10*, 168–175.
15. Obika, S., Nanbu, D., Hari, Y., Morio, K., In, Y., Ishida, T., and Imanishi, T. (1997) Synthesis of 2′-*O*,4′-*C*-methyleneuridine and -cytidine. Novel bicyclic nucleosides having a fixed C3′-endo sugar puckering. *Tetrahedron Lett. 38*, 8735–8738.
16. Obika, S., Nanbu, D., Hari, Y., Andoh, J., Morio, K., Doi, T., and Imanishi, T. (1998) Stability and structural features of the duplexes containing nucleoside analogues with a fixed N-type conformation, 2′-*O*,4′-*C*-methyleneribonucleosides. *Tetrahedron Lett. 39*, 5401–5404.
17. Imanishi, T., and Obika, S. (1999) Syntheses and properties of novel conformationally restrained nucleoside analogues. *J. Syn. Org. Chem. Jpn. 57*, 969–980.
18. Obika, S., Hari, Y., Sugimoto, T., Sekiguchi, M., and Imanishi, T. (2000) Triplex-forming enhancement with high sequence selectivity by single 2′-*O*,4′-*C*-methylene bridged nucleic acid (2′,4′-BNA) modification. *Tetrahedron Lett. 41*, 8923–8927.
19. Torigoe, H., Hari, Y., Sekiguchi, M., Obika, S., and Imanishi, T. (2001) 2′-*O*,4′-*C*-methylene bridged nucleic acid modification promotes pyrimidine motif tripler DNA formation at physiological pH—Thermodynamic and kinetic studies. *J. Biol. Chem. 276*, 2354–2360.
20. Obika, S., Uneda, T., Sugimoto, T., Nanbu, D., Minami, T., Doi, T., and Imanishi, T. (2001) 2′-*O*,4′-*C*-methylene bridged nucleic acid (2′,4′-BNA): Synthesis and triplex-forming properties. *Bioorg. Med. Chem. 9*, 1001–1011.
21. Torigoe, H., Obika, S., and Imanishi, T. (2001) Promotion of triplex formation by 2′-*O*,4′-*C*-methylene bridged nucleic acid (2′,4′-BNA) modification: Thermodynamic and kinetic studies. *Nucleosides, Nucleotides Nucleic Acids 20*, 1235–1238.
22. Singh, S. K., Nielsen, P., Koshkin, A. A., and Wengel, J. (1998) LNA (locked nucleic acids): synthesis and high-affinity nucleic acid recognition. *Chem. Commun.,* 455–456.
23. Koshkin, A. A., Singh, S. K., Nielsen, P., Rajwanshi, V. K., Kumar, R., Meldgaard, M., Olsen, C. E., and Wengel, J. (1998) LNA (Locked Nucleic Acids): Synthesis of the adenine, cytosine, guanine, 5-methylcytosine, thymine and uracil bicyclonucleoside monomers, oligomerisation, and unprecedented nucleic acid recognition. *Tetrahedron 54*, 3607–3630.
24. Singh, S. K., and Wengel, J. (1998) Universality of LNA-mediated high-affinity nucleic acid recognition. *Chem. Commun.,* 1247–1248.
25. Sorensen, M. D., Meldgaard, M., Raunkjaer, M., Rajwanshi, V. K., and Wengel, J. (2000) Branched oligonucleotides containing bicyclic nucleotides as branching points and DNA or LNA as triplex forming branch. *Bioorg. Med. Chem. Lett. 10*, 1853–1856.
26. Sun, B. W., Babu, B. R., Sorensen, M. D., Zakrzewska, K., Wengel, J., and Sun, J. S. (2004) Sequence and pH effects of LNA-containing triple helix-forming oligonucleotides: physical chemistry, biochemistry, and modeling studies. *Biochemistry 43*, 4160–4169.
27. Giovannangeli, C., Diviacco, S., Labrousse, V., Gryaznov, S., Charneau, P., and Helene, C. (1997) Accessibility of nuclear DNA to triplex-forming oligonucleotides: The integrated HIV-1 provirus as a target. *Proc. Natl. Acad. Sci. U.S.A. 94*, 79–84.
28. Gryaznov, S., and Chen, J. K. (1994) Oligodeoxyribonucleotide N3′→P5′ Phosphoramidates—Synthesis and Hybridization Properties. *J. Am. Chem. Soc. 116*, 3143–3144.
29. Gryaznov, S. M., Lloyd, D. H., Chen, J. K., Schultz, R. G., DeDionisio, L. A., Ratmeyer, L., and Wilson, W. D. (1995) Oligonucleotide N3′→P5′ phosphoramidates. *Proc. Natl. Acad. Sci. U.S.A. 92*, 5798–5802.
30. Chen, J. K., Schultz, R. G., Lloyd, D. H., and Gryaznov, S. M. (1995) Synthesis of oligodeoxyribonucleotide N3′→P5′ phosphoramidates. *Nucleic Acids Res. 23*, 2661–2668.
31. Nelson, J. S., Fearon, K. L., Nguyen, M. Q., McCurdy, S. N., Frediani, J. E., Foy, M. F., and Hirschbein, B. L. (1997) N3′→P5′ oligodeoxyribonucleotide phosphoramidates: A new method of synthesis based on a phosphoramidite amine-exchange reaction. *J. Org. Chem. 62*, 7278–7287.
32. Escude, C., Giovannangeli, C., Sun, J. S., Lloyd, D. H., Chen, J. K., Gryaznov, S. M., Garestier, T., and Helene, C. (1996) Stable triple helices formed by oligonucleotide N3′→P5′ phosphoramidates inhibit transcription elongation. *Proc. Natl. Acad. Sci. U.S.A. 93*, 4365–4369.

33. Torigoe, H. (2001) Thermodynamic and kinetic effects of N3′→P5′ phosphoramidate modification on pyrimidine motif triplex DNA formation. *Biochemistry 40*, 1063–1069.
34. Obika, S., Onoda, M., Morita, K., Andoh, J., Koizumi, M., and Imanishi, T. (2001) 3′-amino-2′,4′-BNA: novel bridged nucleic acids having an N3′→P5′ phosphoramidate linkage. *Chem. Commun.,* 1992–1993.
35. Obika, S., Rahman, S. M. A., Song, B., Onoda, M., Koizumi, M., Morita, K., and Imanishi, T. (2008) Synthesis and properties of 3′-amino-2′,4′-BNA, a bridged nucleic acid with a N3′→P5′ phosphoramidate linkage. *Bioorg. Med. Chem. 16*, 9230–9237.
36. Cassidy, S. A., Strekowski, L., Wilson, W. D., and Fox, K. R. (1994) Effect of a triplex-binding ligand on parallel and antiparallel DNA triple helices using short unmodified and acridine-linked oligonucleotides. *Biochemistry 33*, 15338–15347.
37. Maruyama, A., Watanabe, H., Ferdous, A., Katoh, M., Ishihara, T., and Akaike, T. (1998) Characterization of interpolyelectrolyte complexes between double-stranded DNA and polylysine comb-type copolymers having hydrophilic side chains. *Bioconjugate Chem. 9*, 292–299.
38. Maruyama, A., Katoh, M., Ishihara, T., and Akaike, T. (1997) Comb-type polycations effectively stabilize DNA triplex. *Bioconjugate Chem. 8*, 3–6.
39. Ferdous, A., Watanabe, H., Akaike, T., and Maruyama, A. (1998) Poly(L-lysine)-*graft*-dextran copolymer: amazing effects on triplex stabilization under physiological pH and ionic conditions (*in vitro*). *Nucleic Acids Res. 26*, 3949–3954.
40. Ferdous, A., Watanabe, H., Akaike, T., and Maruyama, A. (1998) Comb-type copolymer: Stabilization of triplex DNA and possible application in antigene strategy. *J. Pharm. Sci. 87*, 1400–1405.
41. Torigoe, H., Ferdous, A., Watanabe, H., Akaike, T., and Maruyama, A. (1999) Poly(L-lysine)-*graft*-dextran copolymer promotes pyrimidine motif triplex DNA formation at physiological pH—Thermodynamic and kinetic studies. *J. Biol. Chem. 274*, 6161–6167.
42. Torigoe, H., Ferdous, A., Watanabe, H., Akaike, T., and Maruyama, A. (1999) Poly(L-lysine)-*graft*-dextran copolymer remarkably promotes pyrimidtne-motif triplex formation at neutral pH: Thermodynamic and kinetic studies. *Nucleosides, Nucleotides Nucleic Acids 18*, 1655–1656.
43. Maruyama, A., Ohnishi, Y., Watanabe, H., Torigoe, H., Ferdous, A., and Akaike, T. (1999) Polycation comb-type copolymer reduces counterion condensation effect to stabilize DNA duplex and triplex formation. *Colloids Surf., B 16*, 273–280.
44. Ferdous, A., Akaike, T., and Maruyama, A. (2000) Inhibition of sequence-specific protein-DNA interaction and restriction endonuclease cleavage via triplex stabilization by poly(L-lysine)-*graft*-dextran copolymer. *Biomacromolecules 1*, 186–193.
45. Maruyama, A. (2000) in *Pharmaceutical Aspects of Oligonucleotides* (Couvreur, P., and Malvy, C., Eds.) pp 172−197, Taylor & Francis, London.
46. Sato, Y. I., Kobayashi, Y., Kamiya, T., Watanabe, H., Akaike, T., Yoshikawa, K., and Maruyama, A. (2005) The effect of backbone structure on polycation comb-type copolymer/DNA interactions and the molecular assembly of DNA. *Biomaterials 26*, 703–711.
47. Torigoe, H., and Maruyama, A. (2005) Synergistic stabilization of nucleic acid assembly by oligo-N3′→P5′ phosphoramidate modification and additions of comb-type cationic copolymers. *J. Am. Chem. Soc. 127*, 1705–1710.
48. Bates, P. J., Dosanjh, H. S., Kumar, S., Jenkins, T. C., Laughton, C. A., and Neidle, S. (1995) Detection and kinetic studies of triplex formation by oligodeoxynucleotides using real-time biomolecular interaction analysis (BIA). *Nucleic Acids Res. 23*, 3627–3632.
49. Torigoe, H., Shimizume, R., Sarai, A., and Shindo, H. (1999) Triplex formation of chemically modified homopyrimidine oligonucleotides: thermodynamic and kinetic studies. *Biochemistry 38*, 14653–14659.
50. Manzini, G., Xodo, L. E., Gasparotto, D., Quadrifoglio, F., van der Marel, G. A., and van Boom, J. H. (1990) Triple helix formation by oligopurine-oligopyrimidine DNA fragments. Electrophoretic and thermodynamic behavior. *J. Mol. Biol. 213*, 833–843.
51. Manning, G. S. (1978) The molecular theory of polyelectrolyte solutions with applications to the electrostatic properties of polynucleotides. *Q. Rev. Biophys. 11*, 179–246.
52. Record, M. T., Jr., Anderson, C. F., and Lohman, T. M. (1978) Thermodynamic analysis of ion effects on the binding and conformational equilibria of proteins and nucleic acids: the roles of ion association or release, screening, and ion effects on water activity. *Q. Rev. Biophys. 11*, 103–178.
53. Singleton, S. F., and Dervan, P. B. (1993) Equilibrium association constants for oligonucleotide-directed triple helix formation at single DNA sites: linkage to cation valence and concentration. *Biochemistry 32*, 13171–13179.
54. Hampel, K. J., Crosson, P., and Lee, J. S. (1991) Polyamines favor DNA triplex formation at neutral pH. *Biochemistry 30*, 4455–4459.
55. Thomas, T., and Thomas, T. J. (1993) Selectivity of polyamines in triplex DNA stabilization. *Biochemistry 32*, 14068–14074.
56. Record, M. T., Jr., Lohman, M. L., and De Haseth, P. (1976) Ion effects on ligand-nucleic acid interactions. *J. Mol. Biol. 107*, 145–158.
57. Mascotti, D. P., and Lohman, T. M. (1990) Thermodynamic extent of counterion release upon binding oligolysines to single-stranded nucleic acids. *Proc. Natl. Acad. Sci. U.S.A. 87*, 3142–3146.
58. Olins, D. E., Olins, A. L., and Von Hippel, P. H. (1967) Model nucleoprotein complexes: studies on the interaction of cationic homopolypeptides with DNA. *J. Mol. Biol. 24*, 157–176.
59. Shapiro, J. T., Leng, M., and Felsenfeld, G. (1969) Deoxyribonucleic acid-polylysine complexes. Structure and nucleotide specificity. *Biochemistry 8*, 3219–3232.
60. Haynes, M., Garrett, R. A., and Gratzer, W. B. (1970) Structure of nucleic acid-poly base complexes. *Biochemistry 9*, 4410–4416.
61. Kim, W. J., Ishihara, T., Akaike, T., and Maruyama, A. (2001) Comb-type cationic copolymer expedites DNA strand exchange while stabilizing DNA duplex. *Chem. Eur. J. 7*, 176–180.
62. Kim, W. J., Akaike, T., and Maruyama, A. (2002) DNA strand exchange stimulated by spontaneous complex formation with cationic comb-type copolymer. *J. Am. Chem. Soc. 124*, 12676–12677.
63. Kim, W. J., Sato, Y., Akaike, T., and Maruyama, A. (2003) Cationic comb-type copolymers for DNA analysis. *Nat. Mater. 2*, 815–820.
64. Wu, L. L., Shimada, N., Kano, A., and Maruyama, A. (2008) Poly(L-lysine)-*graft*-dextran copolymer accelerates DNA hybridization by two orders. *Soft Matter 4*, 744–747.
65. Kamiya, M., Torigoe, H., Shindo, H., and Sarai, A. (1996) Temperature dependence and sequence specificity of DNA triplex formation: An analysis using isothermal titration calorimetry. *J. Am. Chem. Soc. 118*, 4532–4538.
66. Rahman, S. M. A., Seki, S., Obika, S., Haitani, S., Miyashita, K., and Imanishi, T. (2007) Highly stable pyrimidine-motif triplex formation at physiological pH values by a bridged nucleic acid analogue. *Angew. Chem., Int. Ed. 46*, 4306–4309.

BI801795Z